

Towards the determination of the 3-dimensional structure of the proton using lattice QCD simulations

Constantia Alexandrou^{1,2,*} and Simone Bacchio^{2,**}

¹Department of Physics, University of Cyprus, PO Box 20537, 1678 Nicosia, Cyprus

²Computation-based Science and Technology Research Center, The Cyprus Institute, 20 Konstantinou Kavafi str., 2121 Aglantzia, Cyprus

Abstract. State-of-the-art lattice QCD simulations enable the evaluation of nucleon form factors and Mellin moments with controlled systematics, yielding results with unprecedented accuracy. At the same time, new theoretical approaches are allowing the direct computation of nucleon generalized parton distributions. We review recent lattice QCD results on these quantities that are paving the way for extracting a wealth of information on the 3-dimensional structure of the nucleon.

1 Introduction

The Lagrangian of the theory of the strong interaction, Quantum Chromodynamics (QCD), was written 50 years ago [1]. Solving it and obtaining quantitative results is very challenging due to the non-perturbative nature of the strong interactions. The lattice formulation provides the non-perturbative framework to regularise the theory [2] and, after rotating to imaginary time, to compute hadronic properties using *ab initio* simulations [3, 4]. The development of powerful computers have helped immensely the field. However, equally important were theoretical and algorithmic breakthroughs [5–7]. Nowadays, simulations are carried out at physical values of the quark masses, large enough lattice size and small enough lattice spacing. New theoretical developments are extending the quantities that can be extracted from such simulations, opening new areas where lattice QCD can provide insights and valuable input to phenomenology and experiments. A particularly relevant theoretical development for determining the structure of the nucleon is the large momentum effective theory (LaMET) [8] that gives access to the direct computation of parton distribution functions (PDFs) and their generalization, the generalized parton distributions (GPDs).

2 State-of-the lattice QCD simulations

In Fig. 1 we show a summary of the zero-temperature gauge ensembles available for hadron structure studies. The three most used discretization fermion schemes are clover-type, staggered and domain wall fermions. All major collaborations have gauge ensembles simulated approximately at the physical value of the pion mass. The Extended Twisted Mass Collaboration (ETMC) completed the simulation of three gauge ensembles at three different lattice spacings using twisted mass clover-improved fermions with the masses of the light, strange and charm quarks tuned close to their physical values. These three ensembles enable the extraction of form factors and Mellin moments taking the continuum limit directly at the physical pion mass, eliminating the need for chiral extrapolations.

*Speaker, e-mail: alexand@ucy.ac.cy

**e-mail: s.bacchio@cyi.ac.cy

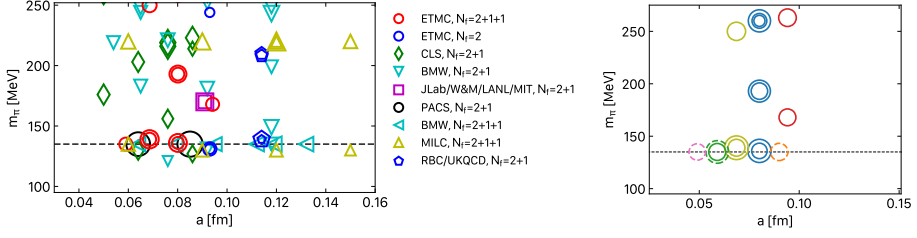


Figure 1. Left: Gauge ensembles by various collaborations using clover improved fermions (ETMC, CLS, BMW, JLab/W&M/LANL/MIT, PACS), staggered fermions (BMW, MILC) and Domain wall fermions (RBC/UKQCD). The size of the symbols reflects the spatial volume of the lattice. Right: Gauge ensembles produced (solid circles) or under production (dashed circles) by ETMC. The dashed horizontal lines show the physical value of the pion mass.

Ensemble	V/a^4	β	a [fm]	m_π [MeV]	$m_\pi L$
cB211.072.64	$64^3 \times 128$	1.778	0.07957(13)	140.2(2)	3.62
cC211.060.80	$80^3 \times 160$	1.836	0.06821(13)	136.7(2)	3.78
cD211.054.96	$96^3 \times 192$	1.900	0.05692(12)	140.8(2)	3.90

Table 1. Parameters for the $N_f = 2 + 1 + 1$ ETMC ensembles. In the first column, we give the name of the ensemble, in the second the lattice volume, in the third $\beta = 6/g^2$ with g the bare coupling constant, in the fourth the lattice spacing, in the fifth the pion mass, and in the sixth the value of $m_\pi L$. Lattice spacings and pion masses are taken from Ref. [9].

3 Axial form factors

The nucleon axial form factors are important quantities for weak interactions, neutrino scattering, and parity violation experiments. Since the value of the nucleon axial charge g_A is well known, it has been used over the years as a benchmark quantity for lattice QCD computations. The nucleon axial charge, g_A , is extracted directly in lattice QCD from the forward matrix element of the axial-vector current. In Fig. 2, we show the continuum limit using the three ETMC ensembles of Table 1. In the continuum limit, we find $g_A = 1.245(28)(14)$, where the first error is statistical and the second the systematic due to excited states. In Fig. 2, we also show results of numerous lattice QCD studies as presented in the 2021 FLAG report [11]. As can be seen, the lattice results reproduce the value of g_A .

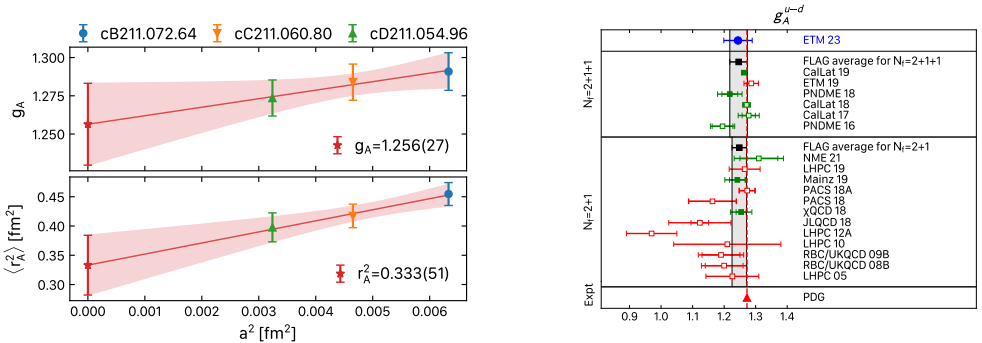


Figure 2. Left: Continuum extrapolation of g_A and the axial radius r_A using the the three ETMC ensembles of Table 1 [10]. Right: Comparison of lattice QCD results on g_A as published by FLAG [11] where we include the ETMC result with the blue circle, labeled ETM 23.

Results for the axial form factors are shown in Fig. 3. We fit the Q^2 -dependence using a dipole form or the z-expansion. From the slope in the continuum limit, we find for the axial radius $\langle r_A^2 \rangle = 0.339(67)(06) \text{ fm}^2$. We also check the pion pole dominance (PPD) hypothesis

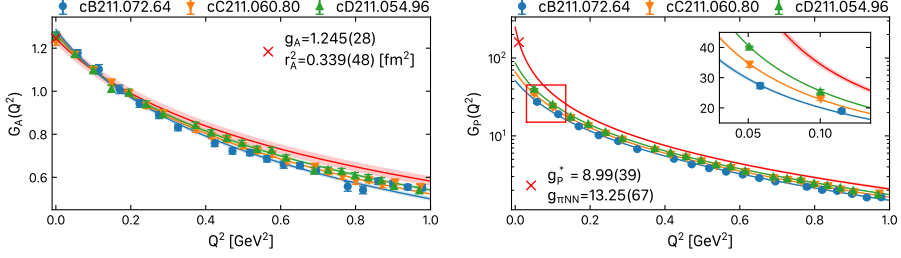


Figure 3. Results on the axial $G_A(Q^2)$ (left) and induced pseudoscalar $G_P(Q^2)$ (right) form factors as a function of Q^2 . The red solid line shows the continuum extrapolation [10].

that predicts that the value of the ratio $G_A(Q^2)/G_P(Q^2)|_{Q^2 \rightarrow -m_\pi^2} = \frac{Q^2 + m_\pi^2}{4m_N^2}$, close to the pole. We take the continuum limit using the Ansatz $f(Q^2, a^2) = c_0 + c_1 Q^2 + c_2 a^2 + c_3 a^2 Q^2$. We find that, in the continuum limit, the slope $c_1 \sim 1/4m_N^2$ and c_0 is consistent with zero, showing that PPD hypothesis is fulfilled, as shown in Fig. 4. A quantity of interest for the induced pseudoscalar form factor is the induced pseudoscalar coupling determined at the muon capture point [12], namely $g_P^* \equiv \frac{m_\mu}{2m_N} G_P(0.88 m_\mu^2)$ with $m_\mu = 105.6$ MeV the muon mass. We find that $g_P^* = 8.99(39)(49)$, which agrees with the value of 8.44(16) obtained in chiral perturbation theory [13]. For a non-zero pion mass, the spontaneous breaking of chiral symmetry relates the axial-vector current to the pion field ψ_π , through the relation $\partial^\mu A_\mu = F_\pi m_\pi^2 \psi_\pi$. In QCD, the axial Ward-Takahashi identity leads to the partial conservation of the axial-vector current (PCAC) $\partial^\mu A_\mu = 2m_q P$, where P is the pseudoscalar operator and $m_q = m_u = m_d$ is the light quark mass for degenerate up and down quarks, where $P = \bar{u}\gamma_5 u - \bar{d}\gamma_5 d$ is the isovector pseudoscalar current. The PCAC relation at the form factors level relates the axial and induced pseudoscalar form factors to the pseudoscalar form factor via the relation

$$G_A(Q^2) - \frac{Q^2}{4m_N^2} G_P(Q^2) = \frac{m_q}{m_N} G_5(Q^2). \quad (1)$$

Using the PCAC relation, it also follows that the pion field can be expressed as $\psi_\pi = \frac{2m_q P}{F_\pi m_\pi^2}$ and one can connect the pseudoscalar form factor to the pion-nucleon form factor $G_{\pi NN}(Q^2)$ as follows[10]

$$m_q G_5(Q^2) = \frac{F_\pi m_\pi^2}{m_\pi^2 + Q^2} G_{\pi NN}(Q^2), \quad (2)$$

which is written so that it illustrates the pole structure of $G_5(Q^2)$ and the preferred usage of $m_q G_5(Q^2)$, which is a scale-independent quantity unlike $G_5(Q^2)$. Substituting $m_q G_5(Q^2)$ in Eq. (1), one obtains the Goldberger-Treiman relation [14, 15]

$$G_A(Q^2) - \frac{Q^2}{4m_N^2} G_P(Q^2) = \frac{F_\pi m_\pi^2}{m_N(m_\pi^2 + Q^2)} G_{\pi NN}(Q^2). \quad (3)$$

The pion-nucleon form factor $G_{\pi NN}(Q^2)$ at the pion pole gives the pion-nucleon coupling $g_{\pi NN} \equiv \lim_{Q^2 \rightarrow -m_\pi^2} G_{\pi NN}(Q^2) = \lim_{Q^2 \rightarrow -m_\pi^2} (Q^2 + m_\pi^2) G_P(Q^2) / 4m_N^2 F_\pi$, where F_π is the pion decay constant. Using the latter relation, we find $g_{\pi NN} = 13.25(67)(69)$. By extracting the nucleon matrix element of the pseudoscalar current we determine the pseudoscalar form factor $G_5(Q^2)$, which has a similarly Q^2 dependence as $G_P(Q^2)$. If PPD is satisfied then the ratio $r_{\text{PPD},2} \equiv \frac{4m_N}{m_\pi^2} \frac{m_q G_5(Q^2)}{G_P(Q^2)} \Big|_{Q^2 \rightarrow -m_\pi^2}$ should be unity. This ratio is shown in Fig. 4 and deviates

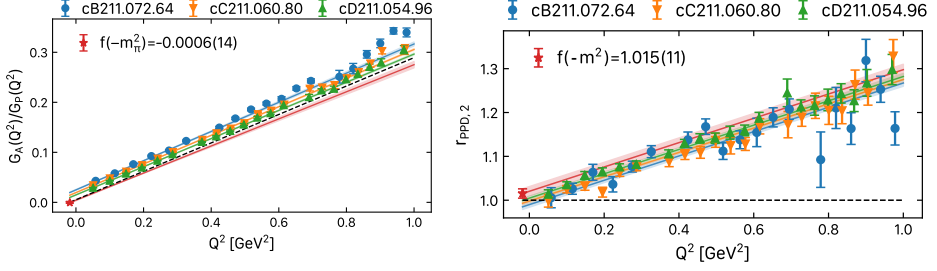


Figure 4. Results on the ratios $G_A(Q^2)/G_P(Q^2)$ (left) and $r_{PP,D,2}$ (right) as a function of Q^2 . The red bands show the continuum extrapolation [10].

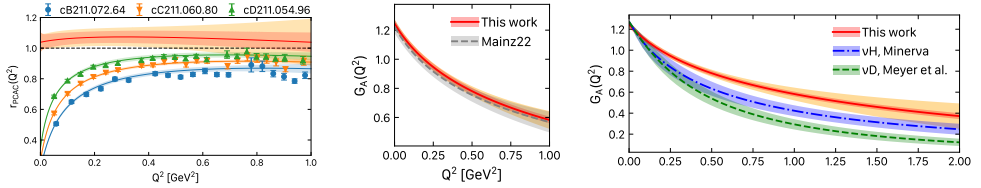


Figure 5. Left: r_{PCAC} for the three ETMC ensembles of Table 1 and in the continuum limit (red band) and when including the systematic error due to excited states (yellow band). The black dashed line is the expected result if PPD is satisfied at any Q^2 . Middle: Comparison of ETMC results with a recent computation by the CLS-Mainz group [16] shown with the gray dashed line with its error band. Right: Comparison of ETMC continuum values on $G_A(Q^2)$ with the fit to the deuterium bubble-chamber data [17] shown by the green dashed line with error band and with the fit to the recent MINER ν A antineutrino-hydrogen data [18] shown by the blue dot-dashed line with error band.

from unity. From the slope one can compute the Goldberger-Treiman deviation Δ_{GT} . We find $\Delta_{GT} = -0.0213(38)$ in agreement with the 2% deviation predicted by chiral perturbation theory [19] and determine the low energy constant $\bar{d}_{18} = g_A \Delta_{GT} / 2m_\pi^2 = -0.73(13) \text{ GeV}^{-2}$. Since PCAC is an exact operator relation, it provides a stringent test of our analysis on the form factor level. Therefore the ratio

$$r_{PCAC}(Q^2) = \frac{\frac{m_q}{m_N} G_5(Q^2) + \frac{Q^2}{4m_N^2} G_P(Q^2)}{G_A(Q^2)}, \quad (4)$$

should be unity if lattice artifacts are correctly accounted for. In Fig. 5, we show r_{PCAC} for the three ETMC ensembles of Table 1. For finite lattice spacing the ratio is not unity. However, when we take the continuum limit the PCAC is satisfied as expected. In Fig. 5 we compare our final value of $G_A(Q^2)$ in the continuum limit with that determined by the CLS-Mainz collaboration. ETMC results are fully compatible with the results of CLS-Mainz and also favor the latest analysis of the MINER ν A antineutrino-hydrogen data [18].

4 Decomposition of the nucleon spin

A surprising result was found by the European Muon Collaboration (EMC) [20, 21] more than 30 years ago, namely that only about half the proton spin was carried by its valence quarks. This triggered numerous experimental and theoretical studies to understand the so-called proton spin puzzle. In lattice QCD the total angular momentum carried by valence and sea quarks and gluons can be computed by evaluating the second Mellin moments [22–24]. We extract these moments by evaluating the nucleon matrix elements of the traceless part of the energy momentum tensor $\bar{T}_{q,g}^{\mu\nu}$. They can be decomposed into generalized form factors

(GFFs) that depend only on the momentum transfer squared q^2 . In Minkowski space we have [25]

$$\langle N(p', s') | \tilde{T}_{q,g}^{\mu\nu} | N(p, s) \rangle = \bar{u}_N(p', s') \left[A_{20}^{q,g}(q^2) \gamma^{\mu} P^{\nu} + B_{20}^{q,g}(q^2) \frac{i\sigma^{\mu\rho} q_{\rho} P^{\nu}}{2m_N} + C_{20}^{q,g}(q^2) \frac{q^{\mu} q^{\nu}}{m_N} \right] u_N(p, s) \quad (5)$$

where u_N is the nucleon spinor with initial (final) momentum $p(p')$ and spin $s(s')$, $P = (p' + p)/2$ is the total momentum and $q = p' - p$ the momentum transfer. $A_{20}^{q,g}(q^2)$, $B_{20}^{q,g}(q^2)$ and $C_{20}^{q,g}(q^2)$ are the three GFFs. In the forward limit, $A_{20}^{q,g}(0)$ gives the quark and gluon average momentum fraction $\langle x \rangle^{q,g}$. Summing over all quark and gluon contributions gives the momentum sum $\langle x \rangle^q + \langle x \rangle^g = 1$. Furthermore, the total spin carried by a quark is given by $J^q = \frac{1}{2} [A_{20}^q(0) + B_{20}^q(0)]$ [26].

In Fig. 6, we show our results for the proton average momentum fraction for the up, down, strange and charm quarks, for the gluons as well as their sum. The up quark makes the largest quark contribution of about 35% and it is twice as big as that of the down quark. The strange quark contributes significantly smaller, namely about 5% and the charm contributes about 2%. The gluon has a significant contribution of about 45%. Summing all the contributions results to $\sum_{q=u,d,s,c} \langle x \rangle_R^{q^+} + \langle x \rangle_R^g = 1.045(118)$ confirming the expected momentum sum. Fig. 6, showing connected and disconnected contributions, demonstrates that disconnected contributions are crucial and if excluded would result to a significant underestimation of the momentum sum.

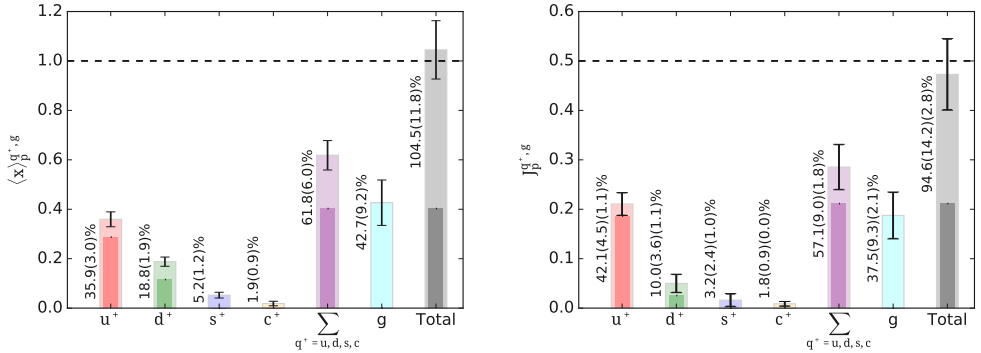


Figure 6. The decomposition of the proton average momentum fraction $\langle x \rangle_p$ (left) and spin J_p . We show the contribution of the up (red bar), down (green bar), strange (blue bar) and charm (orange bar) quarks and their sum (purple bar), the gluon (cyan bar) and the total sum (grey bar). Note that what is shown is the contribution of both the quarks and antiquarks ($q^+ = q + \bar{q}$). Whenever two overlapping bars appear the darker bar denotes the purely connected contribution while the light one is the total contribution, which includes disconnected taking into account also the mixing. The error bars on the only connected part are omitted while for the total are shown explicitly on the bars. The percentages written in the figure are for the total contribution. The dashed horizontal line is the momentum and spin sums. Results are given in $\overline{\text{MS}}$ scheme at 2 GeV.

The individual contributions to the proton spin are presented in Fig. 6. The major contribution comes from the up quark amounting to about 40% of the proton spin. The down, strange and charm quarks have relatively smaller contributions. All quark flavors together constitute to about 60% of the proton spin. The gluon contribution is as significant as that of the up quark, providing the missing piece to obtain $J_p = 94.6(14.2)(2.8)\%$ of the proton spin, confirming indeed the spin sum. The $\sum_{q=u,d,s} B_{20}^{q^+}(0) + B_{20}^g(0)$ is expected to vanish in order to respect the momentum and spin sums. We find for the renormalized values that

$\sum_{q=u,d,s} B_{20,R}^{q^+}(0) + B_{20,R}^g(0) = -0.099(91)(28)$, which is indeed compatible with zero. We note that these results were obtained using the ETMC ensemble CB211.072.64 and are thus not extrapolated to the continuum limit. The computation using the other two ensembles of Table 1 is ongoing.

5 Direct computation of PDFs and GPDs

PDFs are light-cone correlation matrix elements given by

$$F_{\Gamma}(x) = \frac{1}{2} \int \frac{dz^-}{2\pi} e^{ixP^+z^-} \langle N(p) | \bar{\psi}(-z/2) \Gamma W(-z/2, z/2) \psi(z/2) | N(p) \rangle |_{z^+=0, \vec{z}=0}, \quad (6)$$

and as such cannot be computed on a Euclidean lattice. In a pioneering paper, X. Ji[8]

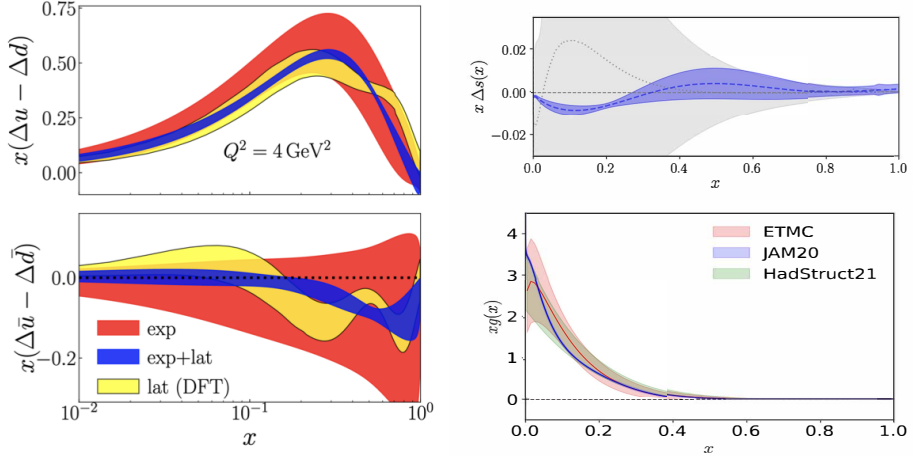


Figure 7. Left: JAM17 results are shown with the red band, lattice QCD results are shown with the yellow band [27] using one ETMC ensemble with physical pion mass, while the blue band shows the combined fits using both lattice and experimental data [28]. Right top: Strange helicity using an ETMC ensemble with pion mass of 260 MeV (blue band) compared to phenomenological analysis (gray band) [29]. Right bottom: A comparison of ETMC results on the gluon PDF [30] (red) with those of of HadStruc [31] (green), and the global analysis of JAM20 [32] (blue). Results are shown in the MS scheme at a scale of 2 GeV.

proposed instead to compute matrix elements of spatial correlators e.g. along the z -axis, and a nucleon state with a large momentum boost in the z -direction. For large enough boosts, one can relate these so called quasi-distributions to the light-cone distributions through a matching kernel computed in perturbation theory. Within this large momentum effective theory (LaMET) one can then extract directly PDFs and, allowing momentum transfers, the GPDs. For PDFs, we compute

$$\tilde{F}_{\Gamma}(x, P_3, \mu) = 2P_3 \int_{-\infty}^{\infty} \frac{dz}{4\pi} e^{-ixP_3z} \langle P_3 | \bar{\psi}(0) \Gamma W(0, z) \psi(z) | P_3 \rangle |_{\mu} \quad (7)$$

and, after non-perturbative renormalization, we match the quasi-PDF $\tilde{F}_{\Gamma}(x, P_3, \mu)$ to extract the PDF

$$\tilde{F}_{\Gamma}(x, P_3, \mu) = \int_{-1}^1 \frac{dy}{|y|} C\left(\frac{x}{y}, \frac{\mu}{yP_3}\right) F_{\Gamma}(y, \mu) + \mathcal{O}\left(\frac{m_N^2}{P_3^2}, \frac{\Lambda_{\text{QCD}}^2}{P_3^2}\right)$$

through the matching kernel $C\left(\frac{x}{y}, \frac{\mu}{yP_3}\right)$. Although these computations are not as mature as the computation of Mellin moments, first results are very promising. In Fig. 7, we show results

on the nucleon isovector helicity from lattice QCD, from the JAM collaboration analysis, and when combined. As can be seen, using lattice QCD input greatly improves the theoretical predictions. In Fig. 7, we also show the gluon PDF computed using pseudo-distributions, a variant of quasi-distributions.

6 Conclusions

Lattice QCD results produce known experimental values of e.g. the nucleon axial charge, and the electromagnetic form factors and, thus, can be reliably used to predict other less known quantities such as the tensor charge, axial form factors, and pseudoscalar form factor providing valuable input to experiments and phenomenology. Second Mellin moments that probe the distribution of spin among the quarks and gluons can be extracted reliably and provide a quantitative understanding of the fraction of the momentum and spin carried by quarks and gluons on the proton. Direct computation of PDFs, GPDs and TMDs can now be computed in lattice QCD and a lot of progress is foreseen in the near future on determining these important quantities that will provide a more complete picture of hadron structure.

Acknowledgments. C.A. acknowledges partial support by the project 3D-nucleon, id number EXCELLENCE/0421/0043, co-financed by the European Regional Development Fund and the Republic of Cyprus through the Research and Innovation Foundation and by the European Joint Doctorate AQTIVATE that received funding from the European Union's research and innovation program under the Marie Skłodowska-Curie Doctoral Networks action and Grant Agreement No 101072344. S.B. is funded by the project QC4LGT, id number EXCELLENCE/0421/0019, co-financed by the European Regional Development Fund and the Republic of Cyprus through the Research and Innovation Foundation.

References

- [1] H. Fritzsch, M. Gell-Mann and H. Leutwyler, *Phys. Lett. B* **47** (1973), 365-368 doi:10.1016/0370-2693(73)90625-4
- [2] K. G. Wilson, *Phys. Rev. D* **10** (1974), 2445-2459 doi:10.1103/PhysRevD.10.2445
- [3] M. Luscher, [arXiv:hep-lat/9802029 [hep-lat]].
- [4] M. Luscher, *Annales Henri Poincaré* **4** (2003), S197-S210 doi:10.1007/s00023-003-0916-z [arXiv:hep-ph/0211220 [hep-ph]].
- [5] M. Luscher, *JHEP* **05** (2003), 052 doi:10.1088/1126-6708/2003/05/052 [arXiv:hep-lat/0304007 [hep-lat]].
- [6] M. Luscher, *Comput. Phys. Commun.* **156** (2004), 209-220 doi:10.1016/S0010-4655(03)00486-7 [arXiv:hep-lat/0310048 [hep-lat]].
- [7] M. Luscher, *Comput. Phys. Commun.* **165** (2005), 199-220 doi:10.1016/j.cpc.2004.10.004 [arXiv:hep-lat/0409106 [hep-lat]].
- [8] X. Ji, *Phys. Rev. Lett.* **110** (2013), 262002 doi:10.1103/PhysRevLett.110.262002 [arXiv:1305.1539 [hep-ph]].
- [9] C. Alexandrou *et al.* [Extended Twisted Mass], *Phys. Rev. D* **107** (2023) no.7, 074506 doi:10.1103/PhysRevD.107.074506 [arXiv:2206.15084 [hep-lat]].
- [10] C. Alexandrou, S. Bacchio, M. Constantinou, J. Finkenrath, R. Frezzotti, B. Kostrzewa, G. Koutsou, G. Spanoudes and C. Urbach, [arXiv:2309.05774 [hep-lat]].
- [11] Y. Aoki *et al.* [Flavour Lattice Averaging Group (FLAG)], *Eur. Phys. J. C* **82** (2022) no.10, 869 doi:10.1140/epjc/s10052-022-10536-1 [arXiv:2111.09849 [hep-lat]].
- [12] J. Egger, D. Fahrni, M. Hildebrandt, A. Hofer, L. Meier, C. Petitjean, V. A. Andreev, T. I. Banks, S. M. Clayton and V. A. Ganzha, *et al.*
- [13] V. Bernard, N. Kaiser and U. G. Meissner, *Phys. Rev. D* **50**, 6899-6901 (1994) doi:10.1103/PhysRevD.50.6899 [arXiv:hep-ph/9403351 [hep-ph]].

- [14] C. Alexandrou, G. Koutsou, T. Leontiou, J. W. Negele and A. Tsapalis, PoS **LATTICE2007** (2007), 162 doi:10.22323/1.042.0162 [arXiv:0710.2173 [hep-lat]].
- [15] C. Alexandrou, G. Koutsou, T. Leontiou, J. W. Negele and A. Tsapalis, Phys. Rev. D **76** (2007), 094511 [erratum: Phys. Rev. D **80** (2009), 099901] doi:10.1103/PhysRevD.80.099901 [arXiv:0706.3011 [hep-lat]].
- [16] D. Djukanovic, G. von Hippel, J. Koponen, H. B. Meyer, K. Ottnad, T. Schulz and H. Wittig, Phys. Rev. D **106** (2022) no.7, 074503 doi:10.1103/PhysRevD.106.074503 [arXiv:2207.03440 [hep-lat]].
- [17] A. S. Meyer, M. Betancourt, R. Gran and R. J. Hill, Phys. Rev. D **93** (2016) no.11, 113015 doi:10.1103/PhysRevD.93.113015 [arXiv:1603.03048 [hep-ph]].
- [18] T. Cai *et al.* [MINERvA], Nature **614** (2023) no.7946, 48-53 doi:10.1038/s41586-022-05478-3
- [19] M. Nagy and M. D. Scadron, Acta Phys. Slov. **54** (2004) no.5, 427-432 [arXiv:hep-ph/0406009 [hep-ph]].
- [20] J. Ashman *et al.* [European Muon], Phys. Lett. B **206** (1988), 364 doi:10.1016/0370-2693(88)91523-7
- [21] J. Ashman *et al.* [European Muon], Nucl. Phys. B **328** (1989), 1 doi:10.1016/0550-3213(89)90089-8
- [22] C. Alexandrou, [arXiv:2112.09038 [hep-lat]].
- [23] C. Alexandrou, S. Bacchio, M. Constantinou, J. Finkenrath, K. Hadjiyiannakou, K. Jansen, G. Koutsou, H. Panagopoulos and G. Spanoudes, Phys. Rev. D **101** (2020) no.9, 094513 doi:10.1103/PhysRevD.101.094513 [arXiv:2003.08486 [hep-lat]].
- [24] C. Alexandrou, M. Constantinou, K. Hadjiyiannakou, K. Jansen, C. Kallidonis, G. Koutsou, A. Vaquero Avilés-Casco and C. Wiese, Phys. Rev. Lett. **119** (2017) no.14, 142002 doi:10.1103/PhysRevLett.119.142002 [arXiv:1706.02973 [hep-lat]].
- [25] X. D. Ji, J. Phys. G **24** (1998), 1181-1205 doi:10.1088/0954-3899/24/7/002 [arXiv:hep-ph/9807358 [hep-ph]].
- [26] X. D. Ji, Phys. Rev. Lett. **78** (1997), 610-613 doi:10.1103/PhysRevLett.78.610 [arXiv:hep-ph/9603249 [hep-ph]].
- [27] C. Alexandrou, K. Cichy, M. Constantinou, K. Jansen, A. Scapellato and F. Steffens, Phys. Rev. Lett. **121** (2018) no.11, 112001 doi:10.1103/PhysRevLett.121.112001 [arXiv:1803.02685 [hep-lat]].
- [28] J. Bringewatt, N. Sato, W. Melnitchouk, J. W. Qiu, F. Steffens and M. Constantinou, Phys. Rev. D **103** (2021) no.1, 016003 doi:10.1103/PhysRevD.103.016003 [arXiv:2010.00548 [hep-ph]].
- [29] C. Alexandrou, M. Constantinou, K. Hadjiyiannakou, K. Jansen and F. Manigrasso, Phys. Rev. Lett. **126** (2021) no.10, 102003 doi:10.1103/PhysRevLett.126.102003 [arXiv:2009.13061 [hep-lat]].
- [30] J. Delmar, C. Alexandrou, K. Cichy, M. Constantinou and K. Hadjiyiannakou, Phys. Rev. D **108** (2023) no.9, 094515 doi:10.1103/PhysRevD.108.094515 [arXiv:2310.01389 [hep-lat]].
- [31] T. Khan *et al.* [HadStruc], Phys. Rev. D **104** (2021) no.9, 094516 doi:10.1103/PhysRevD.104.094516 [arXiv:2107.08960 [hep-lat]].
- [32] E. Moffat *et al.* [Jefferson Lab Angular Momentum (JAM)], Phys. Rev. D **104** (2021) no.1, 016015 doi:10.1103/PhysRevD.104.016015 [arXiv:2101.04664 [hep-ph]].